Nonlinear Reliable Control With Application to a Vehicle Antilock Brake System

Yew-Wen Liang, *Member, IEEE*, Chih-Chiang Chen, Der-Cherng Liaw, *Senior Member, IEEE*, and Yuan-Tin Wei

***Abstract*—This paper explores the design of active reliable control systems for a class of uncertain nonlinear affine systems using an integral-type sliding mode control (ISMC) scheme. The presented scheme not only maintains the main advantages of the ISMC design, including robustness, rapid response and easy implementation, but it can also tolerate some actuator faults when fault detection and diagnosis information is available. In this study, the uncertainties and/or disturbances are not required to be of the matched type; however, when they are matched, the state trajectories of the nominal healthy subsystem and the uncertain faulty system are identical. As a result, engineers can predictively address the matched uncertain faulty system performance in light of the performance of the nominal healthy subsystem. The analytic results are also applied to the study of a vehicle brake reliable control system. Simulation results demonstrate the benefits of the proposed scheme.**

***Index Terms*—Antilock brake system, Reliable control, state-dependent Riccati equation, robustness, integral-type sliding mode control.**

I. Introduction

THE study of reliable (or fault-tolerant) control has recently attracted considerable attention and become of great importance [1]–[16] because it is often not possible to provide repair and maintenance promptly, particularly for the systems in aerospace missions. The main goal of reliable control is to design a controller whose closed-loop system can tolerate the abnormal operation of specific control components while retaining overall system stability with acceptable system performance. Existing reliable design approaches are based on a variety of methods, including coprime factorization [8], the algebraic Riccati equation [9], the linear matrix inequality [10], the Hamilton–Jacobi equation (HJE) [11], [12], sliding mode control (SMC) [13]–[15] and integral-type sliding mode control (ISMC) [16]. Among these reliable control methods, only the HJE, SMC, and ISMC approaches deal with the reliability issues for nonlinear systems. However, because the HJE-based approach is implemented using optimization, reliable controllers using this approach depend on the solution of an associated HJE that is difficult to solve. Although a power series method [17] can reduce the difficulty by using a computer calculation of the HJE, the solution obtained is only an approximation and the computational burden grows quickly when the system is complicated. In contrast, the reliable designs based on SMC or ISMC do not require the solution of an HJE, and they retain the advantages of SMC schemes. These advantages include rapid response, easy implementation, and low sensitivity to model uncertainties and/or external disturbances (MUED) [18].

In addition to having the benefits of the SMC-based schemes mentioned above, the ISMC-based schemes also possess four advantages. First, it has been reported that SMC schemes can be sensitive to MUED during the period when the system state has not yet reached the sliding manifold [19]. Unlike SMC schemes, the system states of ISMC schemes start in the sliding manifold and remain there, which improves robustness. Second, the maximum control magnitude required by ISMC is generally smaller than that by SMC, in which it usually occurs at the beginning of the period before the sliding manifold is reached. Thus, the physical control magnitude constraints imposed by ISMC designs are easier to fulfill than those by SMC designs. Third, the effect of unmatched MUED can be minimized through the selection of sliding manifold parameters [19], [20]. Finally, the state response of the matched uncertain system is identical to that of the nominal system if the system state remains on the sliding manifold. The last property gives engineers greater flexibility in designing an appropriate controller for the nominal system by creating a desired system trajectory for the state of the uncertain system to follow. Thus, the ISMC design allows engineers to predict the performance of the uncertain system, which is in general not easily implemented by other nonlinear control techniques. In light of the many benefits of ISMC schemes, this study will investigate reliable controller design using the ISMC approach. With this approach, engineers can achieve better system performance not only under normal condition but also under a variety of uncertain fault situations. In [16], a reliable control design from the ISMC viewpoint has been exploited. However, it only dealt with a special structure of nonlinear systems. In this paper, we will extend that previous study to those for more general dynamical systems.

The rest of this paper is organized as follows. Section II states the problem and the main goal of this paper. Section III describes the design of the ISMC reliable control law. Section IV

Manuscript received November 28, 2011; revised November 01, 2012; accepted December 07, 2012. Date of publication December 20, 2012; date of current version October 14, 2013. This work was supported by the National Science Council, Taiwan, under Grants NSC 98-2218-E-009-017-, NSC 99-2218-E-009-004-, NSC 100-2221-E-009-026-MY2, and 101-2623-E-009-005-D. Paper no. TII-11-803.

The authors are with the Institute of Electrical and Control Engineering, National Chiao Tung University, Hsinchu 30010, Taiwan (e-mail: ywliang@cn.nctu.edu.tw; ccchen25.ece00g@nctu.edu.tw; ldc@cn.nctu.edu.tw; ywliang@mail.nctu.edu.tw).

Color versions of one or more of the figures in this paper are available online at http://ieeexplore.ieee.org.

Digital Object Identifier 10.1109/TII.2012.2234470

discusses the application of the analytic results to the antilock brake control of a vehicle. Finally, Section V provides the conclusion.

II. Problem Statement

Consider a class of nonlinear uncertain systems described by the following equation:

$$\dot{\mathbf{x}} = \mathbf{f}(\mathbf{x}, t) + G(\mathbf{x}, t)\mathbf{u} + \mathbf{d} \tag{1}$$

where $\mathbf{x} \in \mathcal{R}^n$ and $\mathbf{u} \in \mathcal{R}^m$ denote the system states and the control inputs, respectively, and $\mathbf{d} \in \mathcal{R}^n$ represents the possible MUED, $\mathbf{f}(\mathbf{x}, t) \in \mathcal{R}^n$ and $G(\mathbf{x}, t) \in \mathcal{R}^{n\times m}$. In this work, we will study the design of an active reliable controller for the system (1). We assume that any actuator faults have been detected and diagnosed by a fault detection and diagnosis (FDD) mechanism. The faults considered in this study may be time-varying, which include degradation, amplification and outage [1], [13]. In addition, any type of control strategy meeting the system requirements may be used before a fault happens. After a fault is detected and diagnosed, the control law is guided to switch to an active reliable law to assure good system performance. Thus, after the detection of a fault, we may divide the actuators into two sets, $\mathcal{H}$ and $\mathcal{F}$. We assume that all of the actuators in $\mathcal{H}$ are healthy, while those in $\mathcal{F}$ have undergone faults. The output values of the faulty actuators are expressed as

$$\mathbf{u}_{\mathcal{F}} = \hat{\mathbf{u}}_{\mathcal{F}} + \Delta\mathbf{u}_{\mathcal{F}} \tag{2}$$

where $\hat{\mathbf{u}}_{\mathcal{F}}$ and $\Delta\mathbf{u}_{\mathcal{F}}$ denote the estimated value and the estimation error, respectively, from an FDD mechanism. Let

$$G(\mathbf{x}, t) = (G_{\mathcal{H}}(\mathbf{x}, t)\vdots G_{\mathcal{F}}(\mathbf{x}, t)) \text{ and } \mathbf{u} = \left(\mathbf{u}_{\mathcal{H}}^T \vdots \mathbf{u}_{\mathcal{F}}^T\right)^T \tag{3}$$

where $(\cdot)^T$ denotes the transpose of a vector or a matrix. We assume that $\mathbf{u}_{\mathcal{H}} \in \mathcal{R}^k$, $\mathbf{u}_{\mathcal{F}} \in \mathcal{R}^{m-k}$ and $k < m$. The system in (1) can then be rewritten as

$$\dot{\mathbf{x}} = \mathbf{f}(\mathbf{x}, t) + G_{\mathcal{H}}(\mathbf{x}, t)\mathbf{u}_{\mathcal{H}} + G_{\mathcal{F}}(\mathbf{x}, t)(\hat{\mathbf{u}}_{\mathcal{F}} + \Delta\mathbf{u}_{\mathcal{F}}) + \mathbf{d}. \tag{4}$$

To develop the active reliable controller, we impose the following two assumptions. The first concerns the stabilizability of the nominal healthy subsystem. The other provides a condition that allows the ISMC scheme to be implemented successfully and prevents the need for an unbounded control input.

Assumption 1: There exists a control $\mathbf{u}_{\mathcal{H}0}$ such that the origin of the nominal healthy subsystem

$$\dot{\mathbf{x}} = \mathbf{f}(\mathbf{x}, t) + G_{\mathcal{H}}(\mathbf{x}, t)\mathbf{u}_{\mathcal{H}0} \tag{5}$$

is uniformly asymptotically stable (UAS). That is, there exists a continuously differentiable function $V(\mathbf{x}, t)$ such that

$$\gamma_1(\|\mathbf{x}\|) \le V(\mathbf{x}, t) \le \gamma_2(\|\mathbf{x}\|) \tag{6}$$

and

$$\begin{aligned}\dot{V} &= \frac{\partial V(\mathbf{x}, t)}{\partial t} + \frac{\partial V(\mathbf{x}, t)}{\partial \mathbf{x}} \\ &\quad \cdot [\mathbf{f}(\mathbf{x}, t) + G_{\mathcal{H}}(\mathbf{x}, t)\mathbf{u}_{\mathcal{H}0}] \\ &\le -\gamma_3(\|\mathbf{x}\|)\end{aligned} \tag{7}$$

where $\gamma_1, \gamma_2 : \mathcal{R}^+ \to \mathcal{R}^+$ are class $\mathcal{K}_\infty$ functions and γ_3 is a class $\mathcal{K}$ function [21].

Assumption 2: There exists a constant matrix $D_{\mathcal{H}} \in \mathcal{R}^{k\times n}$ and constant $\sigma_0 > 0$ such that $D_{\mathcal{H}}G_{\mathcal{H}}(\mathbf{x}, t)$ is uniformly invertible in the sense of $\sigma_{\min}(D_{\mathcal{H}}G_{\mathcal{H}}(\mathbf{x}, t)) \ge \sigma_0$ for all nonzero $\mathbf{x}$ and t, where $\sigma_{\min}(\cdot)$ denotes the minimum singular value of a matrix.

Next, we have to distinguish between the matched and the unmatched MUED because at this point, only the actuators in $\mathcal{H}$ are available. In fact, some of the matched MUED for a healthy system may become unmatched due to the occurrence of a fault. Let $(\cdot)^+$ denote the pseudoinverse of a matrix. Then the matched part of $G_{\mathcal{F}}(\mathbf{x}, t)\hat{\mathbf{u}}_{\mathcal{F}}$ in (4) has the form of $G_{\mathcal{H}}(\mathbf{x}, t)G_{\mathcal{H}}^+(\mathbf{x}, t)G_{\mathcal{F}}(\mathbf{x}, t)\hat{\mathbf{u}}_{\mathcal{F}}$, which can be directly compensated by healthy controllers [16], [19]. Thus, the total MUED given by (4) reduce to

$$\mathbf{d}_t := G_{\mathcal{F}}(\mathbf{x}, t)\mathbf{u}_{\mathcal{F}} + \mathbf{d} - G_{\mathcal{H}}(\mathbf{x}, t)G_{\mathcal{H}}^+(\mathbf{x}, t)G_{\mathcal{F}}(\mathbf{x}, t)\hat{\mathbf{u}}_{\mathcal{F}}. \tag{8}$$

Decompose $\mathbf{d}_t$ into its matched and unmatched parts as in (9) below

$$\mathbf{d}_t = G_{\mathcal{H}}(\mathbf{x}, t)\mathbf{d}_m + \mathbf{d}_u \tag{9}$$

where $\mathbf{d}_m = G_{\mathcal{H}}^+(\mathbf{x}, t)\mathbf{d}_t$ and $\mathbf{d}_u = \mathbf{d}_t - G_{\mathcal{H}}(\mathbf{x}, t)\mathbf{d}_m$. Then, by (8) and (9), the system in (4) can be rewritten as

$$\begin{aligned}\dot{\mathbf{x}} = \mathbf{f}(\mathbf{x}, t) &+ G_{\mathcal{H}}(\mathbf{x}, t) \\ &\cdot [\mathbf{u}_{\mathcal{H}} + G_{\mathcal{H}}^+(\mathbf{x}, t)G_{\mathcal{F}}(\mathbf{x}, t)\hat{\mathbf{u}}_{\mathcal{F}} + \mathbf{d}_m] + \mathbf{d}_u.\end{aligned} \tag{10}$$

We impose the next assumption on MUED $\mathbf{d}_m$ and $\mathbf{d}_u$.

Assumption 3: There exist two nonnegative functions $\rho_m(\mathbf{x}, t)$ and $\rho_u(\mathbf{x}, t)$ such that $\|\mathbf{d}_m\| \le \rho_m(\mathbf{x}, t)$ and $\|\mathbf{d}_u\| \le \rho_u(\mathbf{x}, t)$ for all $\mathbf{x}$ and t.

From (8)–(9) and Assumption 3, it is clear that the more accurate the diagnosis of the FDD is, the smaller the functions $\rho_m(\mathbf{x}, t)$ and $\rho_u(\mathbf{x}, t)$ will be. The objective of this study is then to design an appropriate $\mathbf{u}_{\mathcal{H}}$ so that the origin of the closed-loop system is UAS under Assumptions 1–3. It is also worth noting that any other well-developed FDD mechanism can be considered for application here.

III. Reliable Controller Design

To realize the design objective, in this study we will employ the ISMC technique for the design task. According to the ISMC design procedure (see, e.g., [19], [20], and [22]) we introduce the sliding variable as given in (11) below

$$\begin{aligned}\mathbf{s} = \mathbf{s}(\mathbf{x}, t) := D_{\mathcal{H}} \cdot \Big\{ &\mathbf{x}(t) - \mathbf{x}(t_0) \\ &- \int_{t_0}^{t} [\mathbf{f}(\mathbf{x}(\tau), \tau) + G_{\mathcal{H}}(\mathbf{x}(\tau), \tau)\mathbf{u}_{\mathcal{H}0}]\, d\tau \Big\}.\end{aligned} \tag{11}$$

It follows from (10) and (11) that

$$\begin{aligned}\dot{\mathbf{s}} &= D_{\mathcal{H}} \cdot [\dot{\mathbf{x}}(t) - \mathbf{f}(\mathbf{x}, t) - G_{\mathcal{H}}(\mathbf{x}, t)\mathbf{u}_{\mathcal{H}0}] \\ &= D_{\mathcal{H}}G_{\mathcal{H}}(\mathbf{x}, t) \cdot [\mathbf{u}_{\mathcal{H}} + G_{\mathcal{H}}^+(\mathbf{x}, t)G_{\mathcal{F}}(\mathbf{x}, t)\hat{\mathbf{u}}_{\mathcal{F}} \\ &\quad + \mathbf{d}_m - \mathbf{u}_{\mathcal{H}0}] + D_{\mathcal{H}}\mathbf{d}_u.\end{aligned} \tag{12}$$

To maintain the system state on the sliding manifold, we choose

$$\mathbf{u}_{\mathcal{H}} = \begin{cases} \mathbf{u}_{\mathcal{H}0} - G_{\mathcal{H}}^{+}(\mathbf{x},t)G_{\mathcal{F}}(\mathbf{x},t)\hat{\mathbf{u}}_{\mathcal{F}} & \text{if } \mathbf{s} = \mathbf{0}; \\ \mathbf{u}_{\mathcal{H}0} - G_{\mathcal{H}}^{+}(\mathbf{x})G_{\mathcal{F}}(\mathbf{x},t)\hat{\mathbf{u}}_{\mathcal{F}} + \mathbf{u}_{\mathcal{H}1} & \text{if } \mathbf{s} \neq \mathbf{0} \end{cases} \tag{13}$$

where

$$\mathbf{u}_{\mathcal{H}1} = -\rho(\mathbf{x},t)\frac{[D_{\mathcal{H}}G_{\mathcal{H}}(\mathbf{x},t)]^T\mathbf{s}}{\|[D_{\mathcal{H}}G_{\mathcal{H}}(\mathbf{x},t)]^T\mathbf{s}\|} \tag{14}$$

$$\text{and } \rho(\mathbf{x},t) > \rho_m(\mathbf{x},t) + \|[D_{\mathcal{H}}G_{\mathcal{H}}(\mathbf{x},t)]^{-1}D_{\mathcal{H}}\| \cdot \rho_u(\mathbf{x},t). \tag{15}$$

Note that the reliable controller in (13) includes the FDD information. Thus, we can determine the next result.

Theorem 1: Suppose that the system in (1) undergoes actuator faults at the control channels in $\mathcal{F}$ with estimated value $\hat{\mathbf{u}}_{\mathcal{F}}$ and error $\Delta\mathbf{u}_{\mathcal{F}}$ given by (2). Then, under Assumptions 1–3, the origin of the system in (1) with the control law given by (13)–(15) is UAS if

$$\rho_u(\mathbf{x},t) \cdot \left\| \frac{\partial V(\mathbf{x},t)}{\partial \mathbf{x}} \cdot \Gamma(\mathbf{x},t) \right\| < \gamma_3(\|\mathbf{x}\|) \tag{16}$$

for all nonzero $\mathbf{x}$ and t, where

$$\Gamma(\mathbf{x},t) := I_n - G_{\mathcal{H}}(\mathbf{x},t)[D_{\mathcal{H}}G_{\mathcal{H}}(\mathbf{x},t)]^{-1}D_{\mathcal{H}} \tag{17}$$

and I_n denotes the identity matrix of $\mathcal{R}^{n\times n}$.

Proof: From (12)–(15) we have

$$\begin{aligned} \mathbf{s}^T\dot{\mathbf{s}} &= \mathbf{s}^T D_{\mathcal{H}}G_{\mathcal{H}}(\mathbf{x},t) \cdot \{-\mathbf{u}_{\mathcal{H}1} + \mathbf{d}_m \\ &\quad + [D_{\mathcal{H}}G_{\mathcal{H}}(\mathbf{x},t)]^{-1}D_{\mathcal{H}}\mathbf{d}_u\} \\ &\leq \|[D_{\mathcal{H}}G_{\mathcal{H}}(\mathbf{x},t)]^T\mathbf{s}\| \cdot \{-\rho(\mathbf{x},t) + \rho_m(\mathbf{x},t) \\ &\quad + \|[D_{\mathcal{H}}G_{\mathcal{H}}(\mathbf{x},t)]^{-1}D_{\mathcal{H}}\| \cdot \rho_u(\mathbf{x},t)\} \\ &< 0 \end{aligned} \tag{18}$$

for all $\mathbf{s} \neq \mathbf{0}$. Additionally, from (11) we have $\mathbf{s}(\mathbf{x}(t_0),t_0) = \mathbf{0}$. It follows that $\mathbf{s}(\mathbf{x},t) = \mathbf{0}$ for all $t \geq t_0$. That is, the system states remain on the sliding manifold for all $t \geq t_0$. Next, we determine the sliding dynamics (i.e., the motion equations on the sliding manifold) with the aid of the equivalent control method (see, e.g., [18], [19], and [22]). The equivalent control is derived by solving the equation $\dot{\mathbf{s}} = \mathbf{0}$ from (12) as

$$\mathbf{u}_{\mathcal{H}}^{eq} = \mathbf{u}_{\mathcal{H}0} - G_{\mathcal{H}}^{+}(\mathbf{x},t)G_{\mathcal{F}}(\mathbf{x},t)\hat{\mathbf{u}}_{\mathcal{F}} - \mathbf{d}_m - [D_{\mathcal{H}}G_{\mathcal{H}}(\mathbf{x},t)]^{-1}D_{\mathcal{H}}\mathbf{d}_u. \tag{19}$$

By substituting $\mathbf{u}_{\mathcal{H}}^{eq}$ into (10), we have the sliding dynamics

$$\dot{\mathbf{x}} = \mathbf{f}(\mathbf{x},t) + G_{\mathcal{H}}(\mathbf{x},t)\mathbf{u}_{\mathcal{H}0} + \Gamma(\mathbf{x},t)\mathbf{d}_u \tag{20}$$

where $\Gamma(\mathbf{x})$ is given by (17). It then follows from Ineq. (16), (20) and Assumption 1 that

$$\begin{aligned} \dot{V} &\leq -\gamma_3(\|\mathbf{x}\|) + \left\| \frac{\partial V(\mathbf{x},t)}{\partial \mathbf{x}}\Gamma(\mathbf{x},t) \right\| \cdot \rho_u(\mathbf{x},t) \\ &< 0 \end{aligned}$$

for all nonzero $\mathbf{x}$ and t. Thus, the origin is UAS. ■

Remark 1: From the proof of Theorem 1, it is found that the matched MUED can be completely compensated.

Remark 2: Suppose that $G_{\mathcal{H}}(\mathbf{x},t)$ given in (3) is time-invariant, i.e., $G_{\mathcal{H}}(\mathbf{x},t) = G_{\mathcal{H}}(\mathbf{x})$, and $G_{\mathcal{H}}^{\perp}(\mathbf{x}) = \text{span}\{\mathbf{g}_1,\ldots,\mathbf{g}_{n-k}\}$ is involutive, where $G_{\mathcal{H}}^{\perp}(\mathbf{x})$ denotes the orthogonal complement of $G_{\mathcal{H}}(\mathbf{x})$ and $\mathbf{g}_i(\mathbf{x}) \in G_{\mathcal{H}}^{\perp}(\mathbf{x})$ for $i = 1,\ldots,n-k$. Then, by the Frobenius Theorem, there exists a function $\mathbf{h}_{\mathcal{H}} : \mathcal{R}^n \to \mathcal{R}^k$ such that $(\partial\mathbf{h}_{\mathcal{H}}(\mathbf{x}))/(\partial\mathbf{x}) = D_{\mathcal{H}}(\mathbf{x})$ and $D_{\mathcal{H}}(\mathbf{x}) = M(\mathbf{x})G_{\mathcal{H}}^T(\mathbf{x})$ for some nonsingular matrix $M(\mathbf{x}) \in \mathcal{R}^{k\times k}$ [20]. Under such conditions, Rubagotti *et al.* [20] has shown that the matched MUED are completely rejected and the effect of the unmatched MUED is not amplified. That is, $\|\Gamma(\mathbf{x},t)\mathbf{d}_u\| \leq \|\mathbf{d}_u\|$ under the Euclidean norm if the sliding variable $\mathbf{s}$ given by (11) and $\mathbf{u}_{\mathcal{H}1}$ given by (14) are replaced with

$$\mathbf{s} = \mathbf{h}_{\mathcal{H}}(\mathbf{x}) - \mathbf{h}_{\mathcal{H}}(\mathbf{x}_0) - \int_{t_0}^{t} D_{\mathcal{H}}(\mathbf{x}(\tau))[\mathbf{f}(\mathbf{x}(\tau),\tau) + G_{\mathcal{H}}(\mathbf{x}(\tau))\mathbf{u}_{\mathcal{H}0}]d\tau \tag{21}$$

$$\text{and } \mathbf{u}_{\mathcal{H}1} = -\rho(\mathbf{x},t)\frac{[D_{\mathcal{H}}(\mathbf{x})G_{\mathcal{H}}(\mathbf{x})]^T\mathbf{s}}{\|[D_{\mathcal{H}}(\mathbf{x})G_{\mathcal{H}}(\mathbf{x})]^T\mathbf{s}\|}. \tag{22}$$

Moreover, if there exists a constant matrix $B \in \mathcal{R}^{n\times k}$ such that the range spaces spanned by B and $G_{\mathcal{H}}(\mathbf{x})$ are identical, then the functions $\mathbf{h}_{\mathcal{H}}(\mathbf{x})$ and $D_{\mathcal{H}}(\mathbf{x})$ given in (21) can be selected to be $\mathbf{h}_{\mathcal{H}}(\mathbf{x}) = B^T\mathbf{x}$ and $D_{\mathcal{H}}(\mathbf{x}) = B^T$, which also minimizes the effect of the unmatched MUED [20]. Systems in regular form (for the definition, see [20]) clearly have this property, and the matrix B can be easily determined. It follows from the discussions that the ISMC reliable design scheme allows engineers to predictively address the system performance based on the performance of the nominal healthy subsystem. The engineers may use any kind of optimal control action they prefer for the nominal healthy subsystem and also achieve good system performance in uncertain fault situations.

IV. Application to Vehicle Brake Control

This section will demonstrate the use of the reliable scheme in a vehicle brake control application.

A. Vehicle Dynamics

A model of a four-wheeled vehicle was developed by Xiang *et al.* [23]. For simplicity, we consider only the yaw plane motion. The simplified vehicle model in this plane is described in Fig. 1 below with governing equations

$$\dot{V}_x = \frac{1}{m}F_x + \Omega V_y \tag{23}$$

$$\dot{V}_y = \frac{1}{m}F_y - \Omega V_x \tag{24}$$

$$\begin{aligned} I_{zz}\dot{\Omega} &= l_1(L_{fl}c\delta_{\text{sat}} - R_{fl}s\delta_{\text{sat}} + L_{fr}c\delta_{\text{sat}} \\ &\quad - R_{fr}s\delta_{\text{sat}}) - l_3(L_{fl}s\delta_{\text{sat}} + R_{fl}c\delta_{\text{sat}} \\ &\quad - L_{fr}s\delta_{\text{sat}} - R_{fr}c\delta_{\text{sat}} + R_{rl}l_3 - R_{rr}l_3) \\ &\quad - l_2(L_{rl} + L_{rr}) \end{aligned} \tag{25}$$

$$\begin{aligned} F_x &= -(R_{fl} + R_{fr})c\delta_{\text{sat}} - R_{rr} - R_{rl} \\ &\quad - (L_{fl} + L_{fr})s\delta_{\text{sat}} \end{aligned} \tag{26}$$

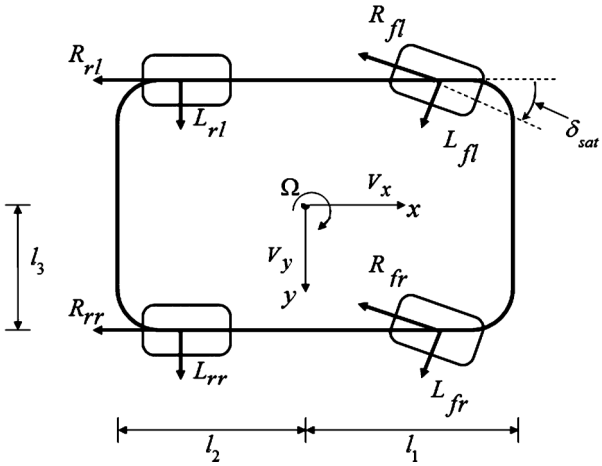

Fig. 1. Front-steering vehicle model.

$$\text{and} \quad F_y = -(R_{fl}+R_{fr})s\delta_{\text{sat}} + L_{rr} + L_{rl} + (L_{fl}+L_{fr})c\delta_{\text{sat}}. \tag{27}$$

Here, the body frame is fixed at the vehicle's center of gravity (CG), and the positive x and y axes represent the forward and rightward directions as observed by the driver. V_x and V_y denote the components of the velocity of the CG in the x and y directions, and Ω is the yaw rate about the vertical z axis. m and I_{zz} are the total mass and the moment of inertia about the vertical axis. F_x and F_y represent the external forces acting on the body along the x and y axes. l_1 and l_2 denote the longitudinal distances from the CG to the front and rear axles, respectively, and l_3 is the lateral distance between the CG and the left or right wheel. L_α and R_α are the lateral and longitudinal forces at each wheel between the tire and the road, where $\alpha = fl, fr, rl, rr$ and the subscripts fl, fr, rl and rr indicate the front-left, front-right, rear-left and rear-right wheels, respectively. δ_{sat} represents the actual output value of the steering wheel angle δ, defined by $\delta_{\text{sat}} = (\pi)/(16)$ if $\delta > (\pi)/(16), \delta_{\text{sat}} = -(\pi)/(16)$ if $\delta < -(\pi)/(16)$ and $\delta_{\text{sat}} = (\pi)/(16) \cdot s\delta$ if $-(\pi)/(16) \le \delta \le (\pi)/(16)$ [26]. Finally, c and s denote the cosine and the sine functions, respectively. To effectively control the vehicle, we have to relate the lateral and longitudinal forces L_α and R_α to the four wheel brake torques and the steering angle, which are considered as the control inputs of this study. Details are given as below.

We adopt L_α and R_α from [24], [25] as follows:

$$L_\alpha = \begin{cases} C_\alpha\left(\delta_{\text{sat}} - \frac{V_y+\Omega l_1}{V_x+\Omega l_3}\right), & \alpha = fl \\ C_\alpha\left(\delta_{\text{sat}} - \frac{V_y+\Omega l_1}{V_x-\Omega l_3}\right), & \alpha = fr \\ C_\alpha\left(\frac{\Omega l_1 - V_y}{V_x+\Omega l_3}\right), & \alpha = rl \\ C_\alpha\left(\frac{\Omega l_1 - V_y}{V_x-\Omega l_3}\right), & \alpha = rr \end{cases} \tag{28}$$

$$\text{and } R_\alpha = \mu_\alpha N_\alpha, \alpha = fl, fr, rl, rr. \tag{29}$$

Here, C_α denotes the cornering stiffness (or lateral stiffness) of the four wheels, $N_{fl} = N_{fr} = (mgl_2)/(2L)$ and $N_{rl} = N_{rr} = (mgl_1)/(2L)$ are normal forces with $L = l_1 + l_2$ and g is the gravity constant. In addition, μ_α defined by

$$\mu_\alpha = [c_1(1 - e^{-c_2\lambda_\alpha}) - c_3\lambda_\alpha] \cdot e^{-c_4\lambda_\alpha V_x} \tag{30}$$

is the tire-road friction coefficient adopted from [25], in which the four parameters c_1, c_2, c_3 and c_4 are introduced by Harifi *et al.* [25] and

$$\lambda_\alpha = \begin{cases} \frac{V_x - r_w\omega_\alpha}{V_x} & \text{during braking;} \\ \frac{V_x - r_w\omega_\alpha}{r_w\omega_\alpha} & \text{during acceleration} \end{cases} \tag{31}$$

are the slip ratios of the four wheels. Finally, r_w and ω_α denote the radius and the angular velocity of the wheels.

To achieve the maximum deceleration of the vehicle, it was suggested by Harifi *et al.* [25] that the wheel slip ratios should track their optimal values λ_α^* for $\alpha = fl, fr, rl$, and rr with which the vehicle will attain maximum traction-control brake force and antilock performance. For this purpose, the dynamics of λ_α is recalled from [25] as given by

$$\dot{\lambda}_\alpha = \frac{\dot{V}_x(1-\lambda_\alpha)}{V_x} + \frac{r_w T_\alpha - \mu_\alpha r_w^2 N_\alpha}{V_x J_w} \tag{32}$$

where J_w and T_α for $\alpha = fl, fr, rl, rr$ denote the wheel's moment of inertia and the four brake torques, respectively. Finally, the steering dynamics are assumed to be (from [26])

$$\tau\dot{\delta} = -\delta + \delta_c \tag{33}$$

where τ is a time constant, and δ and δ_c are the steering angle and its control, respectively.

The overall system dynamics are described by (23)–(25) and (32)–(33), which are in the form of (1) with eight states $[V_x, V_y, \Omega, \delta, \lambda_{fl}, \lambda_{fr}, \lambda_{rl}, \lambda_{rr}]^T$ and five control inputs $[\delta_c, T_{fl}, T_{fr}, T_{rl}, T_{rr}]^T$.

B. ISMC Reliable Scheme

To implement the ISMC reliable scheme, we have to transform the regulation problem into a stabilization problem. For this purpose, we define the tracking error to be $\mathbf{e} = [e_1, e_2, e_3, e_4, e_5, e_6, e_7, e_8]^T = [V_x, V_y, \Omega, \delta, \lambda_{fl} - \lambda_{fl}^*, \lambda_{fr} - \lambda_{fr}^*, \lambda_{rl} - \lambda_{rl}^*, \lambda_{rr} - \lambda_{rr}^*]^T$ and let $\mathbf{u} = [u_1, u_2, u_3, u_4, u_5]^T = [\delta_c, T_{fl}, T_{fr}, T_{rl}, T_{rr}]^T$. Then, the governing (23)–(25) and (32)–(33) in the error states has the form of

$$\dot{\mathbf{e}} = \mathbf{f}(\mathbf{e}) + G(\mathbf{e})\mathbf{u} + \mathbf{d}. \tag{34}$$

Note that (34) is in regular form with

$$G(\mathbf{e}) = [0_{5\times 3}^T, G_1^T(\mathbf{e})_{5\times 5}]^T \tag{35}$$

and $G_1(\mathbf{e}) = \text{diag}\,[1/\tau,\ (r_w)/(e_1 J_w),\ (r_w)/(e_1 J_w),\ (r_w)/(e_1 J_w),\ (r_w)/(e_1 J_w)]$.

To demonstrate the performance of the reliable scheme, we assume in this study that a rear-left brake actuator outage has been detected and diagnosed, i.e., $\mathbf{u}_{\mathcal{H}} = [u_1, u_2, u_3, u_5]^T$ and the output value of $\mathbf{u}_{\mathcal{F}} = [u_4]$ after the fault has been estimated.

Additionally, for simplicity we assume that $N_{fl} = N_{fr} = N_{rl} = N_{rr}, C_{fl} = C_{fr} = C_{rl} = C_{rr}$ and $l_1 = l_2$. To verify Assumption 1, it is observed from (31) that $\lambda_{rl} \approx 0$, because the outage of T_{rl} results in $V_x \approx r_w\omega_\alpha$. After the fault, the forces between the tires and the road should be well distributed to prevent the vehicle from spinning, i.e., the summation of the moments due to the friction forces is expected to vanish. This finding implies that $R_{fl} = R_{fr} + R_{rr}$, where the associated slip ratios can be determined from (29) and (30). For instance, in this example we consider the case of $R_{fl} = R_{fr}$ and $R_{rr} = 0$, i.e., $\lambda^*_{fl} = \lambda^*_{fr} = \lambda^*$ and $\lambda^*_{rl} = \lambda^*_{rr} = 0$, where λ^* denotes the slip ratio that produces the maximum friction force between the tire and road. We now employ the backstepping design method [21] to verify the asymptotic stabilizability of the nominal healthy subsystem. From the structure of (34) and (35), the states e_4, e_5, e_6 and e_8 are controllable, and $e_7 \approx 0$ because the outage of T_{rl}. Thus, by the backstepping design method we only need to find $e_i = \phi_i(e_1, e_2, e_3)$ with $\phi_i(0,0,0) = 0$ for $i = 4, \ldots, 8$ such that $e_j \to 0, j = 1, 2, 3$, when $e_4, \ldots, e_8$ in the first three state equations of (34) are replaced with $\phi_4, \ldots, \phi_8$ and $\mathbf{d} = \mathbf{0}$. To this end, we choose $\phi_i = 0$ for all $i = 4, \ldots, 8$. Then, from (23)–(30) we have $e_1\dot{e}_1 = -(2/m)N_{fl}\cdot\mu^*_{fl}\cdot e_1, e_2\dot{e}_2 = -(4/m)C_{fl}((e_1e_2^2)/(e_1^2 - l_3^2e_3^2))$ and $e_3\dot{e}_3 = -(4)/(I_{zz})C_{fl}((l_1^2e_1e_3^2)/(e_1^2 - l_3^2e_3^2))$, where we have used the facts that $\mu_{rl} = \mu_{rr} = 0, \mu^*_{fl} := \mu_{fl}|_{\lambda_{fl}=\lambda^*}$ and $e_i = \phi_i = 0$ for $i = 4, \ldots, 8$. Note that $e_1 > 0$ unless the vehicle is fully stopped and $\mu^*_{fl} > 0$ because $\lambda^* > 0$. Additionally, it is reasonable to assume that $e_1^2 - l_3^2e_3^3 > 0$ during the braking period because $e_1^2 - l_3^2e_3^3 < 0$ would imply that one of the wheels was moving backward. Thus, $e_i\dot{e}_i < 0$ for all $e_i \neq 0$ and $i = 1, 2, 3$, which result in $e_i \to 0$ for all $i = 1, 2, 3$. By the backstepping method, the origin of the nominal healthy subsystem is found to be UAS and Assumption 1 is verified. Additionally, Assumption 2 is satisfied because the vehicle dynamics given by (34) and (35) are in regular form.

The remaining step is to design a controller $\mathbf{u}_{\mathcal{H}0}$ for the nominal healthy subsystem before and after the fault is detected. It was reported in [26] that the state-dependent Riccati equation (SDRE) design technique, which is known to implement the optimal linear quadratic regulator (LQR) strategy along every nonzero state of the system trajectory, is very efficient in vehicle brake control. Therefore, we adopt the SDRE design as our nominal system controller. Along the SDRE design procedure [27], [28], we select a quadratic performance index in the form of

$$J = \int_0^\infty \left[\mathbf{e}^T Q_{\mathcal{H}}(\mathbf{e})\mathbf{e} + \mathbf{u}_{\mathcal{H}}^T R_{\mathcal{H}}(\mathbf{e})\mathbf{u}_{\mathcal{H}}\right] dt \tag{36}$$

where $Q^T_{\mathcal{H}}(\mathbf{e}) = Q_{\mathcal{H}}(\mathbf{e}) \geq 0$ and $R^T_{\mathcal{H}}(\mathbf{e}) = R_{\mathcal{H}}(\mathbf{e}) > 0$. Then, the drift term should be factorized into the linear structure $\mathbf{f}(\mathbf{e}) = A(\mathbf{e})\mathbf{e}$ having state-dependent coefficients. The SDRE law then has the form

$$\mathbf{u}_{\mathcal{H}0} = -R^{-1}_{\mathcal{H}}(\mathbf{e})G^T_{\mathcal{H}}(\mathbf{e})P(\mathbf{e})\mathbf{e} \tag{37}$$

where $P(\mathbf{e})$ is the solution of the following Riccati equation:

$$A^T(\mathbf{e})P(\mathbf{e}) + P(\mathbf{e})A(\mathbf{e}) - P(\mathbf{e})G_{\mathcal{H}}(\mathbf{e})R^{-1}_{\mathcal{H}}(\mathbf{e})G^T_{\mathcal{H}}(\mathbf{e})P(\mathbf{e}) + Q_{\mathcal{H}}(\mathbf{e}) = 0. \tag{38}$$

Unfortunately, the drift term given by (34) has the property $\mathbf{f}(\mathbf{0}) \neq \mathbf{0}$, which implies that every factorization of $\mathbf{f}(\mathbf{e})$ has a bias term as follows:

$$\mathbf{f}(\mathbf{e}) = A(\mathbf{e})\mathbf{e} + \mathbf{b}(\mathbf{e}) \tag{39}$$

with $\mathbf{b}(\mathbf{0}) \neq \mathbf{0}$. It is also noted that the expression of $A(\mathbf{e})$ is not unique [27]. A set of the expressions for $A(\mathbf{e}), \mathbf{b}(\mathbf{e})$ and $G_{\mathcal{H}}(\mathbf{e})$ are presented in the Appendix. To solve the problem of $\mathbf{f}(\mathbf{0}) \neq \mathbf{0}$, we adopt a strategy from [27] to express $\mathbf{b}(\mathbf{e})$ as $\mathbf{b}(\mathbf{e}) = (\mathbf{b}(\mathbf{e}))/(z) \cdot z$ and augment the system with a stable auxiliary state z as given by (40) below:

$$\dot{z} = -\eta z, \eta > 0. \tag{40}$$

Here, η is selected to be small and $z(0) \neq 0$ so that z changes slowly, and $(\mathbf{b}(\mathbf{e}))/(z)$ is defined and smooth during the control period. With these settings and the augmented error states defined as $\mathbf{e}_a := [\mathbf{e}^T, z]^T$, the augmented system formed by (40) and the nominal healthy subsystem becomes

$$\dot{\mathbf{e}}_a = A_a(\mathbf{e}_a)\mathbf{e}_a + G_{\mathcal{H}a}(\mathbf{e}_a)\mathbf{u}_{\mathcal{H}}, \tag{41}$$

where

$$A_a(\mathbf{e}_a) = \begin{bmatrix} A(\mathbf{e}) & \frac{\mathbf{b}(\mathbf{e})}{z} \\ \mathbf{0}_{1\times 8} & -\eta \end{bmatrix} \quad \text{and } G_{\mathcal{H}a}(\mathbf{e}_a) = \begin{bmatrix} G_{\mathcal{H}}(\mathbf{e}) \\ \mathbf{0} \end{bmatrix}. \tag{42}$$

The SDRE scheme is now performed using the system in (41) with weighting matrices $Q_{\mathcal{H}a}(\mathbf{e}_a) := \text{diag}[Q_{\mathcal{H}}(\mathbf{e}), 0]$ and $R_{\mathcal{H}a}(\mathbf{e}_a) := R_{\mathcal{H}}(\mathbf{e})$. The SDRE controller is modified to be

$$\mathbf{u}_{\mathcal{H}0} = -R^{-1}_{\mathcal{H}}(\mathbf{e})G^T_{\mathcal{H}a}(\mathbf{e}_a)P_a(\mathbf{e}_a)\mathbf{e}_a \tag{43}$$

where $P_a(\mathbf{e}_a)$ is the solution of (38) with $A(\mathbf{e}), G_{\mathcal{H}}(\mathbf{e})$ and $Q_{\mathcal{H}}(\mathbf{e})$ being replaced by $A_a(\mathbf{e}_a), G_{\mathcal{H}a}(\mathbf{e}_a)$ and $Q_{\mathcal{H}a}(\mathbf{e}_a)$.

C. FDD Mechanism

To detect and diagnose the actuator fault for the active reliable controller, we assume that all the state variables are available for measurement or estimation, which is feasible for vehicles [29]. Because the vehicle dynamics given by (34) and (35) are in regular form, we may adopt an observer and the associated residual signals r_i from [15] as below

$$\dot{\zeta}_i = f_{i+3}(\mathbf{e}) + \theta_i u_i + k_i(e_{i+3} - \zeta_i) \tag{44}$$

$$\text{and } r_i = e_{i+3} - \zeta_i \tag{45}$$

for $1 \leq i \leq 5$, where $\theta_1 = (1)/(\tau)$ and $\theta_i = (r_w)/(e_1J_w)$ for $2 \leq i \leq 5$. Additionally, $k_i > 0$ for all $1 \leq i \leq 5$, and f_i and e_i denote the ith entries of $\mathbf{f}$ and $\mathbf{e}$, respectively. It was shown by Liang *et al.* [15] that the observer proposed in (44)–(45) can realize fault detection, fault isolation and fault identification of any single actuator fault. The actual weighting output of the faulty actuator, say $\theta_i u_i^*$, is estimated to be $\theta_i u_i + k_i r_i$, where u_i is the output value we designed the actuator to be, and the diagnosis error was shown to converge to zero at an exponential rate k_i [15]. It should be noted that the FDD is available unless $e_1 = 0$, i.e., the vehicle is fully stopped.

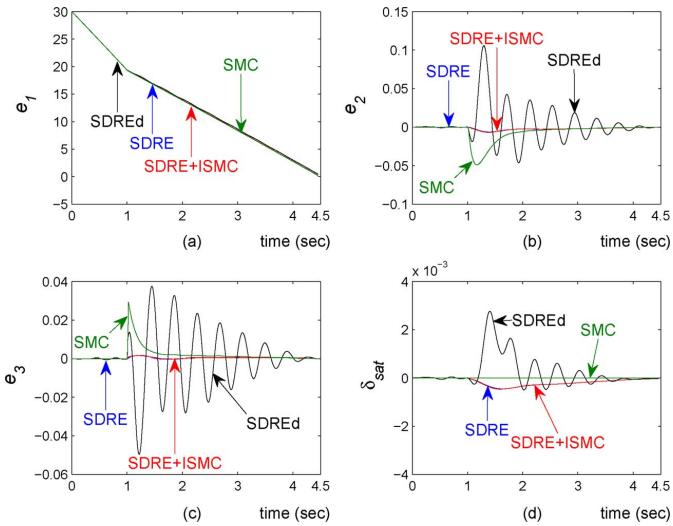

Fig. 2. Time history of the first four error states.

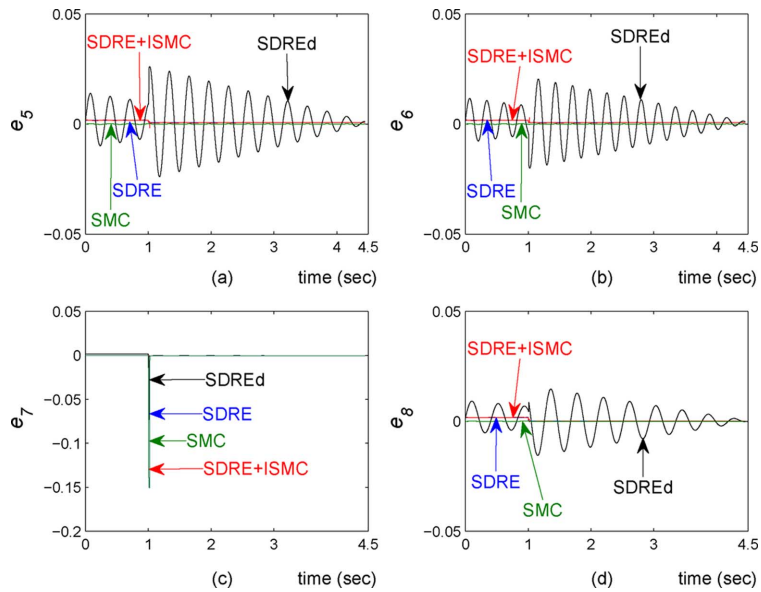

Fig. 3. Time history of the last four error states.

D. Simulation Results

We assume in this example that the rear-left brake actuator experiences outage after one second of braking action, which might result from the abnormal operation of the inverter, braking system and/or wheel motor [30]. Thus, $\mathbf{u}_{\mathcal{H}} = [\delta_c, T_{fl}, T_{fr}, T_{rl}, T_{rr}]^T$ and $\mathbf{u}_{\mathcal{H}} = [\delta_c, T_{fl}, T_{fr}, T_{rr}]^T$ before and after the fault is detected, respectively. The vehicle parameters are adopted from [23] as $m = 1300$ kg, $I_{zz} = 2000$ kgm^2, $l_1 = l_2 = 1.25$ m, $l_3 = 0.8$ m, $C_{fl} = C_{fr} = C_{rl} = C_{rr} = 40000$ N/rad, $r_w = 0.3$ m, $J_w = 0.3$ kgm^2 and $\tau = 30$. The road is assumed to be dry and the Burckhardt tire model parameters are selected to be $c_1 = 1.2801, c_2 = 23.99, c_3 = 0.52$ and $c_4 = 0.02$ for all of the four wheels [25]. Additionally, we assume that the initial states $\mathbf{e}(0) = [30, 0, 0, 10^{-4}, 0, 0, 0, 0]$ and during braking the wheels undergo harmonic MUED with $\mathbf{d} = [0, 0, 0, 0, 21s(20t), 17s(23t), 0, 13s(15t)]^T$.

The control parameters are selected as follows. From the regular form structure of the vehicle dynamics and Remark 2 we select $D_{\mathcal{H}} = [\mathbf{0}_{5\times 3}\ I_{5\times 5}]$ and $D_{\mathcal{H}} = [\mathbf{0}_{4\times 3}\ \boldsymbol{\xi}_1\ \boldsymbol{\xi}_2\ \boldsymbol{\xi}_3\ \mathbf{0}_{4\times 1}\ \boldsymbol{\xi}_4]$ before and after the fault is detected, respectively, where $\{\boldsymbol{\xi}_1, \boldsymbol{\xi}_2, \boldsymbol{\xi}_3, \boldsymbol{\xi}_4\}$ denotes the standard basis of $\mathcal{R}^4$. Before the fault, we choose $\lambda^*_{fl} = \lambda^*_{fr} = \lambda^*_{rl} = \lambda^*_{rr} = \lambda^* = 0.15$. After the fault is detected and diagnosed, we choose $\lambda^*_{fl} = \lambda^*_{fr} = \lambda^* = 0.15$ and $\lambda^*_{rl} = \lambda^*_{rr} = 0$ as mentioned in Section IV-B. Additionally, $\rho_m(\mathbf{e}, t)$ and $\rho(\mathbf{e}, t)$ given in Assumption 3 and (14) are set to be $\rho(\mathbf{e}, t) = \rho_m(\mathbf{e}, t) = \|G^+_{\mathcal{H}}(\mathbf{e})\| \cdot \|\mathbf{d}\|_\infty$, where $\|\mathbf{d}\|_\infty := \sup_t \|\mathbf{d}\|$. To alleviate chatter, the control $\mathbf{u}_{\mathcal{H}1}$ given by (14) is replaced by $\rho(\mathbf{e}, t)([D_{\mathcal{H}} G_{\mathcal{H}}(\mathbf{e})]^T \mathbf{s})/(\epsilon)$ whenever $\|[D_{\mathcal{H}} G_{\mathcal{H}}(\mathbf{e})]^T \mathbf{s}\| \leq \epsilon$ with $\epsilon = 10^{-3}$. The SDRE control parameters are set to be $\eta = 0.001, z(0) = 1000, R_{\mathcal{H}}(\mathbf{e}) = \text{diag}[1, 10^{-3}, 10^{-3}, 10^{-3}, 10^{-3}]$ and $Q_{\mathcal{H}}(\mathbf{e}) = \text{diag}[10^{-6}, 0, 0, 0, 10^7, 10^7, 10^7, 10^7]$ before the fault and set to $R_{\mathcal{H}}(\mathbf{e}) = \text{diag}[1, 10^{-3}, 10^{-3}, 10^{-3}]$ and $Q_{\mathcal{H}}(\mathbf{e}) = \text{diag}[10^{-6}, 0, 0, 0, 10^6, 10^6, 0, 10^6]$ after the fault is

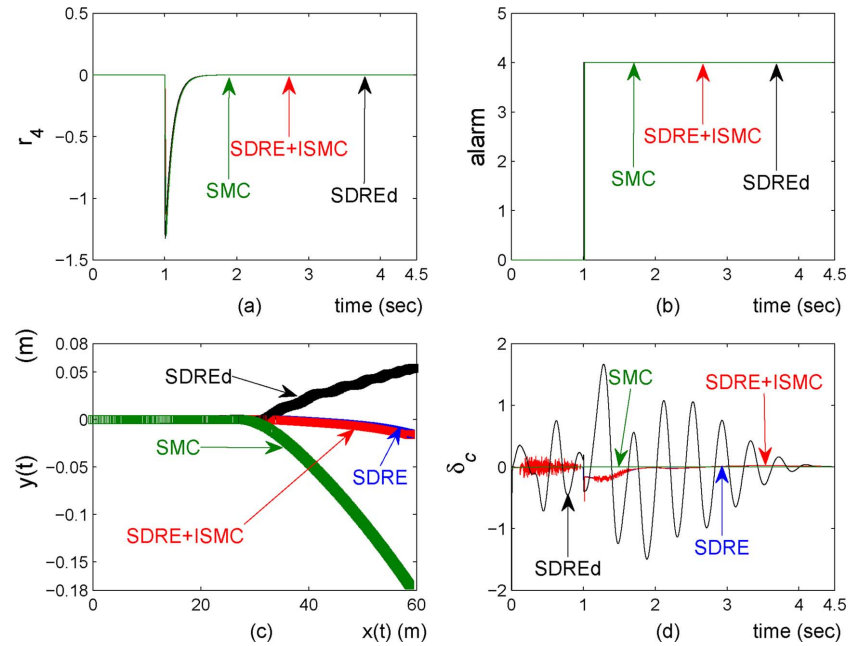

Fig. 4. Time history of (a) residual signals of r_4, (b) alarm signals, (c) vehicle trajectories in the inertial frame and (d) δ_c.

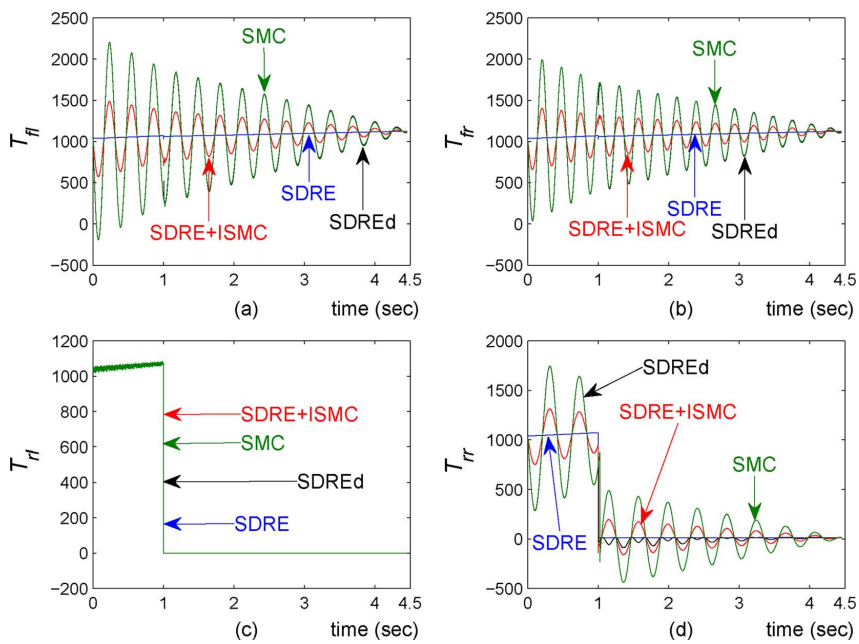

Fig. 5. Time history of the four brake torques.

detected. To compare with the existing reliable designs, in this example we also adopt the sliding mode reliable scheme from [13], as given by (46) below

$$\mathbf{u}_{\mathcal{H}} = (D_{\mathcal{H}} \cdot G_{\mathcal{H}}(\mathbf{e}))^{-1}\{-D_{\mathcal{H}} \cdot \mathbf{f}(\mathbf{e}) - \Lambda_{\mathcal{H}} \cdot \mathrm{sgn}(\mathbf{s})\}. \quad (46)$$

Here, $\mathbf{s}$ and $\Lambda_{\mathcal{H}}$ are chosen to be $\mathbf{s} = [e_4, e_5, e_6, e_7, e_8]^T$ and $\Lambda_{\mathcal{H}} = \mathrm{diag}[10^{-3}, \sup_t |d_5| + 10, \sup_t |d_6| + 10, 60, \sup_t |d_8| + 10]$ before the fault is detected; $\mathbf{s} = [e_4, e_5, e_6, e_8]^T$ and $\Lambda_{\mathcal{H}} = \mathrm{diag}[10^{-3}, \sup_t |d_5| + 10, \sup_t |d_6| + 10, \sup_t |d_8| + 10]$ after the fault is detected and diagnosed, where d_i denotes the ith entry of $\mathbf{d}$. Besides, to alleviate the chatter, the sign function is replaced by the saturation function with boundary layer width 10^{-4}. Finally, the parameters of the FDD observer are chosen to be $k_i = 10$ for all $i = 1, \ldots, 5$, and the threshold of the residual signals for the alarm is set to be 1.3. That is, the alarm is triggered if the magnitude of any of the residual signals from the observer is greater than 1.3.

Here, we consider the following four cases: the first two use the SDRE scheme for the nominal system (labeled SDRE) and the uncertain system (labeled SDREd), whereas the other two use the sliding mode reliable scheme [13] (labeled SMC) and the combination of the SDRE and the ISMC schemes (labeled SDRE + ISMC) for the uncertain system. For better system performance, the SDRE scheme switches to its reliable controller (i.e., the SDRE law for the faulty system) directly

at $t = 1$ without FDD information, whereas the other three are guided to switch to their reliable laws according to the FDD information. Numerical results are depicted in Figs. 2–5. It is observed from Fig. 2(a) that the longitudinal velocity converges to zero for all of the four cases. However, from Figs. 2(b)–(d), the lateral velocity, yaw rate and steering angle of SDREd are found to be much larger than those of the SDRE and SDRE + ISMC and exhibit oscillations that might result in undesirable instability. The same scenario of SDREd can also be observed in Fig. 3 for the remaining error states except e_7, which is 0 because of the outage of T_{rl}. After the fault happens, the lateral velocity and yaw rate of SMC are also found from Figs. 2(b) and (c) to be larger than those of SDRE and SDRE + ISMC, but they decrease to zero soon after the activation of reliable controller. From Figs. 2 and 3, the system states of SDRE and SDRE+ISMC are found to be close to each other, which agrees with the main theoretical results. In Fig. 4(a), the actuator fault is successfully detected by the SDRE + ISMC, SMC and SDREd schemes because the magnitudes of their respective fourth residual signals r_4 exceed the threshold near $t_{\mathrm{SDRE+ISMC}} \approx t_{\mathrm{SDREd}} \approx 1.005$ sec and $t_{\mathrm{SMC}} \approx 1.02$ sec. The success of fault detection can also be observed from the alarm signals given in Fig. 4(b), where the alarm value of 4 denotes the fault of the fourth actuator. After the fault is successfully detected and diagnosed, the associated active reliable controllers are activated, and the magnitude of the residual signals soon decreases, as shown in Fig. 4(a). Fig. 4(c) shows the vehicle trajectories under the four different control schemes. Again, the trajectories of SDRE and SDRE+ISMC are close to each other and exhibit smaller deviations from the centerline than the trajectory of the SMC and SDREd scheme. The associated control curves are displayed in Figs. 4(d) and 5, where the magnitudes of the controls of SDRE + ISMC are found to be smaller than those of SMC and SDREd scheme, except for T_{rr} of SDREd after the fault is detected. These control curves show that the SDRE + ISMC requires less energy than SMC and SDREd before fault happens, while after the fault happens, the ISMC has the ability to intelligently adjust the distribution of its controls so that its state responses are close to those of SDRE. Finally, the quadratic performance given by (36) and the required maximum control magnitude $\|\mathbf{u}\|_\infty := \sup_t \|\mathbf{u}\|_\infty$ of SDRE + ISMC are also found to be better than those of SMC and SDREd in the following relation: $J_{\mathrm{SDRE}} = 1.169 \times 10^4 < J_{\mathrm{SDRE+ISMC}} = 1.182 \times 10^4 < J_{\mathrm{SMC}} = 1.425 \times 10^4 < J_{\mathrm{SDREd}} = 1.505 \times 10^4$ and $(\|\mathbf{u}\|_\infty)_{\mathrm{SDRE}} = 1.125 \times 10^3 < (\|\mathbf{u}\|_\infty)_{\mathrm{SDRE+ISMC}} = 1.486 \times 10^3 < (\|\mathbf{u}\|_\infty)_{\mathrm{SMC}} = 2.202 \times 10^3 < (\|\mathbf{u}\|_\infty)_{\mathrm{SDREd}} = 2.204 \times 10^3$. From this example, it is concluded that the results by using ISMC reliable scheme are more robust and effective than those by SMC or SDRE scheme alone, particularly in the presence of MUED and actuator faults. Moreover, the ISMC reliable scheme provides the designer with freedom in the choice of the nominal controller for better system performance.

V. Conclusion

An active ISMC reliable scheme was presented in this paper for a class of uncertain nonlinear affine systems, which is extended from the previous study for a class of second-order systems [16]. The reliable scheme was shown to be able to tolerate some of actuator faults while maintaining the main advantages of SMC reliable schemes. Additionally, the MUED are not restricted to be of the matched type, and some of the matched MUED may become unmatched because of actuator faults. It was shown that the matched MUED are completely rejected, while the effect of unmatched MUED is not amplified if the control input matrix is time-invariant and the sliding variable parameters are appropriately selected. As a result, engineers may predictably address system performance under both healthy condition and uncertain fault situations. An application example demonstrating vehicle antilock brake reliable control was also presented to demonstrate the benefits of the reliable scheme.

Appendix

The values of $A(\mathbf{e}), \mathbf{b}(\mathbf{e})$ and $G_{\mathcal{H}}(\mathbf{e})$ for (39) and (42) are given below.

Let $A(\mathbf{e}) = [a_{ij}] \in \mathcal{R}^{8\times 8}$. We have $a_{i1} = a_{4j} = a_{2k} = 0$ for $i = 1, \ldots, 8, j = 1, 2, 3, 5, 6, 7, 8$ and $k = 7, 8$. The remaining coefficients of a_{ij} are given as follows:

$$a_{12} = \frac{s\delta_{\mathrm{sat}}}{m}\left(\frac{C_{fl}}{e_1 + l_3 e_3} + \frac{C_{fr}}{e_1 - l_3 e_3}\right);$$

$$a_{13} = \frac{s\delta_{\mathrm{sat}}}{m}\left(\frac{C_{fl} l_1}{e_1 + l_3 e_3} + \frac{C_{fr} l_1}{e_1 - l_3 e_3}\right) + e_2;$$

$$a_{14} = -\frac{\delta_{\mathrm{sat}}(C_{fl} + C_{fr}) s\delta_{\mathrm{sat}}}{m e_4}; \quad a_{15} = -\frac{E_1 c\delta_{\mathrm{sat}}}{m};$$

$$a_{16} = -\frac{E_2 c\delta_{\mathrm{sat}}}{m}; \quad a_{17} = -\frac{E_3}{m}; \quad a_{18} = -\frac{E_4}{m};$$

$$a_{22} = -\frac{1}{m}\left(\frac{C_{fl} c\delta_{\mathrm{sat}} + C_{rl}}{e_1 + l_3 e_3} + \frac{C_{fr} c\delta_{\mathrm{sat}} + C_{rr}}{e_1 - l_3 e_3}\right);$$

$$a_{23} = -\frac{1}{m}\left(\frac{l_1(C_{fl} c\delta_{\mathrm{sat}} + C_{rl})}{e_1 + l_3 e_3} + \frac{l_2(C_{fr} c\delta_{\mathrm{sat}} + C_{rr})}{e_1 - l_3 e_3}\right) - e_1; a_{24} = \frac{\delta_{\mathrm{sat}}(C_{fl} + C_{fr}) c\delta_{\mathrm{sat}}}{m e_4};$$

$$a_{25} = -\frac{E_1 s\delta_{\mathrm{sat}}}{m}; \quad a_{26} = -\frac{E_2 s\delta_{\mathrm{sat}}}{m};$$

$$a_{32} = \frac{C_{fl}(l_3 s\delta_{\mathrm{sat}} - l_1 c\delta_{\mathrm{sat}}) + C_{rl} l_2}{I_{zz}(e_1 + l_3 e_3)} - \frac{C_{fr}(l_1 c\delta_{\mathrm{sat}} + l_3 s\delta_{\mathrm{sat}}) - C_{rr} l_2}{I_{zz}(e_1 - l_3 e_3)};$$

$$a_{33} = \frac{C_{fl}(l_1 l_3 s\delta_{\mathrm{sat}} - l_1^2 c\delta_{\mathrm{sat}}) - C_{rl} l_2^2}{I_{zz}(e_1 + l_3 e_3)} - \frac{C_{fr}(l_1^2 c\delta_{\mathrm{sat}} + l_1 l_3 s\delta_{\mathrm{sat}}) + C_{rr} l_2^2}{I_{zz}(e_1 - l_3 e_3)};$$

$$a_{34} = \frac{l_1 \delta_{\mathrm{sat}}(C_{fl} + C_{fr}) c\delta_{\mathrm{sat}}}{e_4 I_{zz}} + \frac{l_3 \delta_{\mathrm{sat}}(C_{fr} - C_{fl}) s\delta_{\mathrm{sat}}}{e_4 I_{zz}};$$

$$a_{3k} = -\frac{E_{k-4}}{I_{zz}}(l_1 s\delta_{\mathrm{sat}} + l_3 c\delta_{\mathrm{sat}}) \text{ for } k = 5, 6;$$

$$a_{3k} = -\frac{(-1)^k E_{k-4} l_3}{I_{zz}} \text{ for } k = 7, 8; \quad a_{44} = -\frac{1}{\tau};$$

$$a_{52} = \frac{(1 - e_5 - \lambda_{fl}^*) s\delta_{\mathrm{sat}}}{m e_1}\left(\frac{C_{fl}}{e_1 + l_3 e_3} + \frac{C_{fr}}{e_1 - l_3 e_3}\right);$$

$$a_{53} = \frac{(1 - e_5 - \lambda_{fl}^*) s\delta_{\mathrm{sat}}}{m e_1}\left(\frac{C_{fl} l_1}{e_1 + l_3 e_3} + \frac{C_{fr} l_1}{e_1 - l_3 e_3}\right)$$

$$+\frac{(1-e_5-\lambda_{fl}^*)e_2}{e_1};$$

$$a_{54}=-\frac{\delta_{\rm sat}(1-e_5-\lambda_{fl}^*)(C_{fl}+C_{fr})s\delta_{\rm sat}}{me_1e_4};$$

$$a_{55}=-\frac{E_1(1-e_5-\lambda_{fl}^*)c\delta_{\rm sat}}{me_1}+\frac{-r_w^2E_1}{e_1J_w};$$

$$a_{56}=-\frac{E_2(1-e_5-\lambda_{fl}^*)c\delta_{\rm sat}}{me_1};$$

$$a_{5k}=-\frac{E_{k-4}(1-e_5-\lambda_{fl}^*)}{me_1}\ \text{for}\ k=7,8;$$

$$a_{62}=\frac{(1-e_6-\lambda_{fr}^*)s\delta_{\rm sat}}{me_1}\left(\frac{C_{fl}}{e_1+l_3e_3}+\frac{C_{fr}}{e_1-l_3e_3}\right);$$

$$a_{63}=\frac{(1-e_6-\lambda_{fr}^*)s\delta_{\rm sat}}{me_1}\left(\frac{C_{fl}l_1}{e_1+l_3e_3}+\frac{C_{fr}l_1}{e_1-l_3e_3}\right)+\frac{(1-e_6-\lambda_{fr}^*)e_2}{e_1};$$

$$a_{64}=-\frac{\delta_{\rm sat}(1-e_6-\lambda_{fr}^*)(C_{fl}+C_{fr})s\delta_{\rm sat}}{me_1e_4};$$

$$a_{65}=-\frac{E_1(1-e_6-\lambda_{fr}^*)c\delta_{\rm sat}}{me_1};$$

$$a_{66}=-\frac{E_2(1-e_6-\lambda_{fr}^*)c\delta_{\rm sat}}{me_1}+\frac{-r_w^2E_2}{e_1J_w};$$

$$a_{6k}=-\frac{E_{k-4}(1-e_6-\lambda_{fr}^*)}{me_1}\ \text{for}\ k=7,8;$$

$$a_{72}=\frac{(1-e_7-\lambda_{rl}^*)s\delta_{\rm sat}}{me_1}\left(\frac{C_{fl}}{e_1+l_3e_3}+\frac{C_{fr}}{e_1-l_3e_3}\right);$$

$$a_{73}=\frac{(1-e_7-\lambda_{rl}^*)s\delta_{\rm sat}}{me_1}\left(\frac{C_{fl}l_1}{e_1+l_3e_3}+\frac{C_{fr}l_1}{e_1-l_3e_3}\right)+\frac{(1-e_7-\lambda_{rl}^*)e_2}{e_1};$$

$$a_{74}=-\frac{\delta_{\rm sat}(1-e_7-\lambda_{rl}^*)(C_{fl}+C_{fr})s\delta_{\rm sat}}{me_1e_4};$$

$$a_{75}=-\frac{E_1(1-e_7-\lambda_{rl}^*)c\delta_{\rm sat}}{me_1};$$

$$a_{76}=-\frac{E_2(1-e_7-\lambda_{rl}^*)c\delta_{\rm sat}}{me_1};$$

$$a_{77}=-\frac{E_3(1-e_7-\lambda_{rl}^*)}{me_1}+\frac{-r_w^2E_3}{e_1J_w};$$

$$a_{78}=-\frac{E_4(1-e_7-\lambda_{rl}^*)}{me_1};$$

$$a_{82}=\frac{(1-e_8-\lambda_{rr}^*)s\delta_{\rm sat}}{me_1}\left(\frac{C_{fl}}{e_1+l_3e_3}+\frac{C_{fr}}{e_1-l_3e_3}\right);$$

$$a_{83}=\frac{(1-e_8-\lambda_{rr}^*)s\delta_{\rm sat}}{me_1}\left(\frac{C_{fl}l_1}{e_1+l_3e_3}+\frac{C_{fr}l_1}{e_1-l_3e_3}\right)+\frac{(1-e_8-\lambda_{rr}^*)e_2}{e_1};$$

$$a_{84}=-\frac{\delta_{\rm sat}(1-e_8-\lambda_{rr}^*)(C_{fl}+C_{fr})s\delta_{\rm sat}}{me_1e_4};$$

$$a_{85}=-\frac{E_1(1-e_8-\lambda_{rr}^*)c\delta_{\rm sat}}{me_1};$$

$$a_{86}=-\frac{E_2(1-e_8-\lambda_{rr}^*)c\delta_{\rm sat}}{me_1};$$

$$a_{87}=-\frac{E_3(1-e_8-\lambda_{rr}^*)}{me_1};$$

$$a_{88}=-\frac{E_4(1-e_8-\lambda_{rr}^*)}{me_1}+\frac{-r_w^2E_4}{e_1J_w};$$

$$E_k=-N_\alpha c_3e^{-c_4(\lambda_\alpha^*+e_{k+4})e_1}\quad for\ k=1,2,3,4,$$

where $\alpha=fl,fr,rl$ and rr if $k=1,2,3$ and $4,$ respectively.

In addition, let $\mathbf{b}(\mathbf{e})=[b_1,\ldots,b_8]^T$. we have $b_4=0$ and the remaining coefficients of b_i are given as follows:

$$b_1=-\frac{(E_5+E_6)c\delta_{\rm sat}+E_7+E_8}{m};$$

$$b_2=-\frac{(E_5+E_6)s\delta_{\rm sat}}{m};$$

$$b_3=\frac{-l_1(E_5+E_6)s\delta_{\rm sat}-l_3(E_5-E_6)c\delta_{\rm sat}-l_3(E_7-E_8)}{I_{zz}};$$

$$b_k=-\frac{(1-e_k-\lambda_\alpha^*)[(E_5+E_6)c\delta_{\rm sat}+E_7+E_8]}{me_1}+\frac{-r_w^2E_k}{e_1J_w}$$

for $k=5,6,7,8,$ where $\alpha=fl,fr,rl$andrr if $k=5,6,7$ and $8,$ respectively.

$$E_k=N_\alpha c_1e^{-c_4(\lambda_\alpha^*+e_k)e_1}\left(1-e^{-c_2(\lambda_\alpha^*+e_k)}\right)-\lambda_\alpha^*N_\alpha c_3e^{-c_4(\lambda_\alpha^*+e_k)e_1}\ \text{for}\ k=5,6,7,8,$$

where $\alpha=fl,fr,rl$ and rr if $k=5,6,7$ and $8,$ respectively.

Moreover, before a fault, $G_{\mathcal{H}}(\mathbf{e})=G(\mathbf{e})\in\mathcal{R}^{8\times5}$ as given in (35). After the fault is detected, $G_{\mathcal{H}}(\mathbf{e})\in\mathcal{R}^{8\times4}$, which is obtained from $G(\mathbf{e})$ by deleting the fourth column.

REFERENCES

[1] R. F. Stengel, "Intelligent failure-tolerant control," *IEEE Control Syst. Mag.* , vol. 11, no. 4, pp. 14–23, 1991.

[2] S. X. Ding, P. Zhang, S. Yin, and E. L. Ding, "An integrated design framework of fault tolerant wireless networked control systems for industrial automatic control applications," *IEEE Trans. Ind. Inf.*, vol. 9, no. 1, pp. 462–471, Feb. 2013.

[3] P. Panagi and M. M. Polycarpou, "A coordinated communication scheme for distributed fault tolerant control," *IEEE Trans. Ind. Inf.*, vol. 9, no. 1, pp. 386–393, Feb. 2013.

[4] J. Yao, X. Liu, G. Zhu, and L. Sha, "NetSimplex: Controller fault tolerance architecture in networked control systems," *IEEE Trans. Ind. Inf.*, vol. 9, no. 1, pp. 346–356, Feb. 2013.

[5] C. H. Lo, E. H. K. Fung, and Y. K. Wong, "Intellignet automatic fault detection for actuator faulures in aircraft," *IEEE Trans. Ind. Inf.*, vol. 5, no. 1, pp. 50–55, Feb. 2009.

[6] M. H. Kim, S. Lee, and K. C. Lee, "Kalman predictive redundancy system for fault-tolerancy of safety-critical systems," *IEEE Trans. Ind. Inf.*, vol. 6, no. 1, pp. 46–53, Feb. 2010.

[7] X. Liu, Q. Wang, S. Gopalakrishnan, W. He, L. Sha, H. Ding, and K. Lee, "Orgeta: An effcient and flexible online fault tolerance architecture for real-time control systems," *IEEE Trans. Ind. Inf.*, vol. 4, no. 4, pp. 213–224, Nov. 2008.

[8] M. Vidyasagar and N. Viswanadham, "Reliable stabilization using a multi-controller configuration," *Automatica*, pp. 599–602, 1985.

[9] R. J. Veillette, J. V. Medanic, and W. R. Perkins, "Design of reliable control systems," *IEEE Trans. Autom. Control*, vol. 37, no. 3, pp. 290–304, Mar. 1992.

[10] F. Liao, J. L. Wang, and G.-H. Yang, "Reliable robust flight tracking control: An LMI approach," *IEEE Trans. Control Syst. Technol.*, vol. 10, no. 1, pp. 76–89, Jan. 2002.

[11] Y.-W. Liang, D.-C. Liaw, and T.-C. Lee, "Reliable control of nonlinear systems," *IEEE Trans. Autom. Control*, vol. 45, no. 4, pp. 706–710, Apr. 2000.

[12] G.-H. Yang, J. L. Wang, and Y. C. Soh, "Reliable guaranteed cost control for uncertain nonlinear systems," *IEEE Trans. Autom. Control*, vol. 45, no. 11, pp. 2188–2192, Nov. 2000.

[13] Y.-W. Liang and S.-D. Xu, "Reliable control of nonlinear systems via variable structure scheme," *IEEE Trans. Autom. Control*, vol. 51, no. 10, pp. 1721–1725, Oct. 2006.
[14] Y.-W. Liang, S.-D. Xu, and L.-W. Ting, "T-S model-based SMC reliable design for a class of nonlinear control systems," *IEEE Trans. Ind. Electron.*, vol. 56, no. 9, pp. 3286–3295, Sep. 2009.
[15] Y.-W. Liang, S.-D. Xu, and C.-L. Tsai, "Study of VSC reliable designs with application to spacecraft attitude stabilization," *IEEE Trans. Control Syst. Technol.*, vol. 15, no. 2, pp. 332–338, Feb. 2007.
[16] Y.-W. Liang, L.-W. Ting, and L.-G. Lin, "Study of reliable control via an integral-type sliding mode control scheme," *IEEE Trans. on Ind. Electron.*, vol. 59, no. 8, pp. 3062–3068, Aug. 2012.
[17] J. Huang and C.-F. Lin, "Numerical approach to computing nonlinear control laws," *J. Guidance, Contr., Dynamics*, vol. 18, no. 5, pp. 989–994, 1995.
[18] V. I. Utkin, *Sliding Modes in Control and Optimizations*. Berlin, Germany: Springer-Verlag, 1992.
[19] F. Castaños and L. Fridman, "Analysis and design of integral sliding manifolds for systems with unmatched perturbations," *IEEE Trans. Autom. Control*, vol. 51, no. 5, pp. 853–858, May 2006.
[20] M. Rubagotti, A. Estrada, F. Castaños, A. Ferrara, and L. Fridman, "Integral sliding mode control for nonlinear systems with matched and unmatched perturbations," *IEEE Trans. Autom. Control*, vol. 56, no. 11, pp. 2699–2704, Nov. 2011.
[21] H. K. Khalil, *Nonlinear System*, 3rd ed. Englewood Cliffs, NJ, USA: Prentice Hall, 2002.
[22] W.-J. Cao and J.-X. Xu, "Nonlinear integral-type sliding surface for both matched and unmatched uncertain systems," *IEEE Trans. Autom. Control*, vol. 49, no. 8, pp. 1355–1360, Aug. 2004.
[23] W. D. Xiang, P. C. Richardson, C. M. Zhao, and S. Mohammad, "Automobile brake-by-wire control system design and analysis," *IEEE Trans. Veh. Techno.* , vol. 57, no. 1, pp. 138–145, Feb. 2008.
[24] L. Li, F.-Y. Wang, and Q. Zhou, "Integrated longitudinal and lateral tire/road friction modeling and monitoring for vehicle motion control," *IEEE Trans. Intell. Trans. Syst.*, vol. 7, no. 1, pp. 1–19, Mar. 2006.
[25] A. Harifi, A. Aghagolzadeh, G. Alizadeh, and M. Sadeghi, "Designing a sliding mode controller for slip control of antilock brake systems," *Transp. Res. Part C-Emerging Technol.*, vol. 16, no. 6, pp. 731–741, 2008.
[26] T. Acarman, "Nonlinear optimal integrated vehicle control using individual braking torque and steering angle with on-line control allocation by using state-dependent Riccati equation technique," *Veh. Syst. Dynamics*, vol. 47, pp. 155–177, 2009.
[27] T. Cimen, "State-Dependent Riccatif Equation (SDRE) control: A survey," in *Proc. 17th IFAC World Congree*, Seoul, Korea, 2008, vol. 17, pp. 3761–3775.
[28] Y.-W. Liang and L.-G. Lin, "On factorization of the nonlinear drift term for SDRE approach," in *Proc. 18th IFAC World Congree*, Milano, Italy, 2011, pp. 9607–9612.
[29] W. Cho, J. Yoon, S. Yim, B. Koo, and K. Yi, "Estimation of tire forces for application to vehicle stability control," *IEEE Trans. Vehic. Technol.*, vol. 59, no. 2, pp. 638–649, Feb. 2010.
[30] H. Yang, V. Cocquempot, and B. Jiang, "Optimal fault-tolerant patht racking control for 4WS4WD electrical vehicles," *IEEE Trans. Intell. Trans. Syst.*, vol. 11, no. 1, pp. 237–243, Jan. 2010.

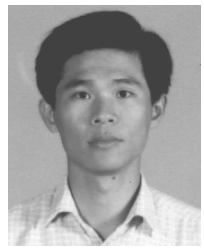

Yew-Wen Liang (M'02) was born in Taiwan, in 1960. He received the B.S. degree in mathematics from the Tung Hai University, Taichung, Taiwan, in 1982, the M.S. degree in applied mathematics, in 1984, and the Ph.D. degree in electrical and control engineering in 1998 from the National Chiao Tung University, Hshinchu, Taiwan, in 1998.

Since August 1987, he has been with the National Chiao Tung University, where he is currently an Associate Professor of Electrical and Control Engineering. His research interests include nonlinear control systems, reliable control, and fault detection and diagnosis issues.

Chih-Chiang Chen received the B.S. degree in electrical engineering from National Yunlin University of Science and Technology (NYUST), Douliou, Taiwan, in 2009, and M.S. degree in electrical and control engineering from National Chiao Tung University, Hshinchu, Taiwan, in 2011. He is currently working toward the Ph.D. degree.

His research interests include nonlinear control systems, reliable control, and fault detection and diagnosis.

Der-Cherng Liaw (S'86–M'90–SM'02) received the B.S. degree in control engineering from National Chiao Tung University (NCTU), Hsinchu, Taiwan, in 1982, the M.S. degree in electrical engineering from National Taiwan University, Taipei, Taiwan, in 1985, and the Ph.D. degree in electrical engineering from the University of Maryland, College Park, MD, USA, in 1990.

During 1990–1991, he was a Postdoctoral Fellow with the Institute of Systems Research, University of Maryland. Since August 1991, he has been with the NCTU, Hsinchu, where he is currently a Professor of electrical and control engineering. During 1994–1995, he was the Director of the Institute of Control Engineering, National Chiao Tung University. His research interests include nonlinear control systems, bifurcation control, applications to jet engine control, flight control, electric power systems and power electronics, RFID, electric vehicle, network based distributive control, and implementation issues.

During 1990–1992, Dr. Liaw served as a Designated Assistant to the Associate Editor for the IEEE TRANSACTIONS ON AUTOMATIC CONTROL. Dr. Liaw was also a Member of Editorial Board of 1993 American Control Conference.

Yuan-Tin Wei received the B.S. degree in mechanical engineering from National Taiwan University of Science and Technology (NTUST), Taipei, Taiwan, in 2007, and the M.S. degree in electrical engineering and control engineering from National Chiao Tung University, Hsinchu, Taiwan, in 2010.

His research interests include control systems, fault detection and diagnosis issues, and vehicle control. He is currently a Software Engineer at ASUSTOR Inc.